



J. Serb. Chem. Soc. 87 (12) 1409–1423 (2022)
JSCS-5603

Journal of the Serbian Chemical Society

JSCS@tmf.bg.ac.rs • www.shd.org.rs/JSCS

Original scientific paper
Published 14 December 2022

Anticorrosion activity of 2-thiohydantoin–Shiff base derivatives for mild steel in 0.5 M HCl

PETAR B. STANIĆ¹, NATAŠA M. VUKIĆEVIĆ^{2*}, VESNA S. CVETKOVIĆ^{2#},
MIROSLAV M. PAVLOVIĆ^{2#}, SILVANA B. DIMITRIJEVIĆ³, BILJANA ŠMIT^{1**}
and MARIJA D. ŽIVKOVIĆ^{4***}

¹*Institute for Information Technologies Kragujevac, University of Kragujevac, Jovana Cvijića bb, 34000 Kragujevac, Serbia*, ²*Institute of Chemistry, Technology and Metallurgy, University of Belgrade, Njegoševa 12, 11000 Belgrade, Serbia*, ³*Mining and Metallurgy Institute Bor, Zeleni bulevar 35, 19210 Bor, Serbia* and ⁴*Faculty of Medical Sciences, University of Kragujevac, Svetozara Markovića 69, 34000 Kragujevac, Serbia*

(Received 12 April, revised 12 July, accepted 24 August 2022)

Abstract: Several 2-thiohydantoin–Shiff base derivatives were prepared as eco-friendly corrosion inhibitors for mild steel in acid environment. Their anticorrosion properties were studied on mild steel in 0.5 M HCl solution as corrosion electrolyte by using usual gravimetric and different electrochemical techniques (weight loss measurement, potentiodynamic polarization and potentiostatic electrochemical impedance spectroscopy). Mild steel surface was characterized using two analytical techniques, scanning electron microscopy for surface morphology and elemental composition and atomic force microscopy. The study has shown that the inhibiting action of these environmentally benign inhibitors synthesized from inexpensive commercially available starting materials could be attributed to adsorption on the metal surface.

Keywords: inhibitors; electrochemistry; surface; potentiodynamic polarization.

INTRODUCTION

As corrosion scourges the production of most industries globally, rising financial costs take their toll. According to a report from 2016, the cost of mitigating the effects of corrosion is estimated to US\$ 2.5 trillion, which amounts to about 3.4 % of the global gross domestic product.¹ Mild steel (MS) is a widely used construction material employed in many industries due to its exemplary mechanical properties and substantially low cost. Despite of its attractive properties and uses, low corrosion resistance of mild steel in acidic solutions notably limits its applications.² Aggressive mineral acid solutions are often used in ind-

* Corresponding authors. E-mail: (*)biljana.smit@uni.kg.ac.rs; (**)mzivkovic@kg.ac.rs

Serbian Chemical Society member.

<https://doi.org/10.2298/JSC220412071S>

ustrial processes which apply mild steel, most notably HCl for acidifying, pickling and industrial cleaning. Corrosion inhibitors are the most practical and profitable way of abating corrosion of metals in aqueous media.^{3–7} Molecules with conjugated multiple bonds, aromatic groups and various atoms like oxygen, sulfur and nitrogen display good corrosion inhibiting activities since they are readily adsorbed on metal surfaces.⁸ But, due to adverse effects on the environment, many of these compounds cannot be used.⁹ Environmental awareness, as well as the ever-rising demand of industry necessitates the use of new, safe, environmentally friendly corrosion inhibitors.^{10–16}

2-Thiohydantoins are derivatives of hydantoins in which a carbonyl group has been replaced with a thiocarbonyl group.¹⁷ They are a class of mostly non-toxic, biologically active drug-based compounds with many applications in medicine and industry.¹⁸ Hydantoin, 2-thiohydantoin and some of their derivatives have displayed some anticorrosion properties.^{19–22} Schiff base molecules that contain the azomethine group have also been shown to exhibit anticorrosion activities.^{23–26} Keeping this in mind, the aim of this study is to explore the corrosion behaviour of four 2-thiohydantoin–Schiff base derivatives, synthesized from inexpensive and commercially available substrates as budget- and eco-friendly corrosion inhibitors, using gravimetric, electrochemical and microscopic methods.

EXPERIMENTAL

Materials and methods

All substrates and reagents were obtained commercially and used without further purification. Solvents were refined by distillation and standard drying procedure before use. IR spectra were recorded on a Perkin-Elmer FT-IR spectrometer model Spectrum One. NMR spectra were recorded on a Varian Gemini 2000 NMR spectrometer in DMSO as the solvent.

Synthesis of inhibitor compounds 1–4

A mixture of aldehyde (0.01 mol) and thiosemicarbazide (0.01 mol) in methanol (30 ml) was refluxed for 3 h and then cooled. The formed precipitate was filtered off, dried, and purified by re-crystallization with hot methanol, yielding thiosemicarbazone. A mixture of thiosemicarbazone (0.01 mol), ethyl chloroacetate (0.01 mol) and anhydrous sodium acetate (0.03 mol) in methanol (50 mL) was refluxed for 6 h. The mixture was cooled and poured into cold water. The resulting precipitate was filtered off, washed with hot water, dried and re-crystallized with hot methanol. The 2-thiohydantoin derivatives are fully characterized by NMR and IR spectroscopy. Spectral data is given in the Supplementary material to this paper.

Preparation of corrosion solutions

The corrosive electrolyte used for electrochemical experiments was 0.5 M HCl, prepared from a 37 % HCl solution diluted with Milli-Q water. Four synthesized 2-thiohydantoin derivatives, compounds 1–4, used in five different concentrations (0.05, 0.1; 0.5, 1.0 and 10 mM) were tested as corrosion inhibitors for MS. Fresh test solutions were prepared by dissolving compounds 1–4 in 0.5 M HCl prior to each experiment.

Electrochemical measurements

The electrochemical measurements were carried out in a three-electrode Pyrex glass cell, where a saturated calomel electrode (SCE), with a Luggin capillary placed close to the working electrode (WE) to compensate the ohmic drop, was used as a reference electrode. All reported potentials were referred to the SCE. The counter electrode was a Pt plate. Mild steel (MS), of chemical composition (mass %) expressed as: Fe with C (max. 0.17 %), P (0.045 %), S (0.045 %), N (0.009 %) was used as the WEs. The MS cylinders were embedded in epoxy resin, leaving a surface area of 1.3 cm^2 exposed to the corrosive acidic solution. Before each experiment WEs were mechanically abraded using silicon carbide paper (grade 600–1200), followed by washing with Milli-Q water in an ultrasonic bath for 5 min, whereupon it was thoroughly rinsed with absolute ethanol and deionized water and finally dried. All experiments were performed at room temperature and without stirring.

Before any electrochemical measurement, the WEs were immersed into the prepared electrolyte for 30 min until a relatively stable open circuit potential (E_{OCP}) was achieved. The typical OCP *vs.* time diagram is shown in Fig. 1; it can be observed that after 30 min of immersion, only negligible changes in the E_{OCP} are measured, showing that the steady-state is achieved after 30 min.

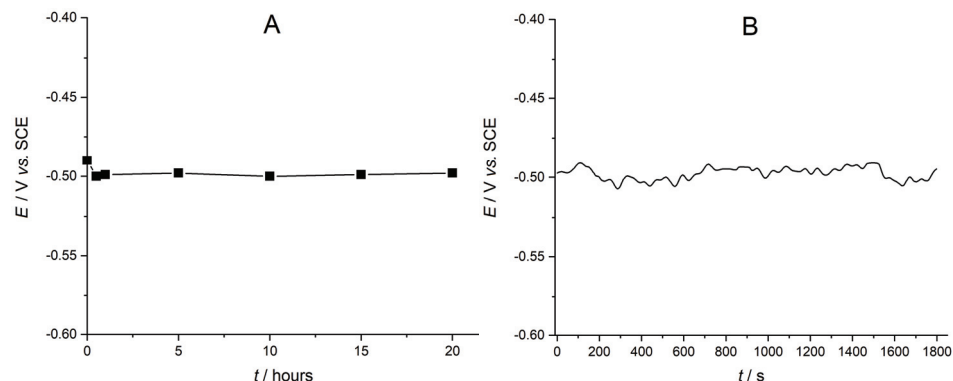


Fig. 1. Open circuit potential curves for MS corrosion in 0.5 M hydrochloric acid solution after 20 h (A) and 30 min (B) of immersion.

Potentiostat/galvanostat EG&G PAR 2631A, controlled by Power Suite software, was used for potentiodynamic polarization (PP) measurements. The PP curves were obtained by changing the potential between -0.250 V and 0.250 V relative to the E_{OCP} with a scan rate of 1 mV s^{-1} .

Potentiostatic electrochemical impedance spectroscopy (PEIS) measurements were performed on potentiostat/galvanostat station BioLogic SAS SP-240 equipped with software for corrosion and physical electrochemistry. PEIS studies were carried out in the frequency range of 10^{-2} – 10^6 Hz by using a 10 mV root mean square sinusoidal potential amplitude around open circuit readings (being in the range from -0.430 to -0.476 V) for all the samples. Randle's equivalent circuit was employed for fitting and analysis of the PEIS data using Zview® software.

Gravimetric measurements

MS weight loss test was performed in a 200 mL beaker with 100 mL of the test solution in the absence and the presence of different inhibitor concentrations. Before testing, MS cylinder samples were polished, thoroughly rinsed with absolute ethanol and deionized water, dried and weighted. Then, the samples were inserted in the test solutions for 24 h. All experiments were triplicated in order to reach a good reliability. Average weight loss in the absence and in the presence of inhibitor was reported.

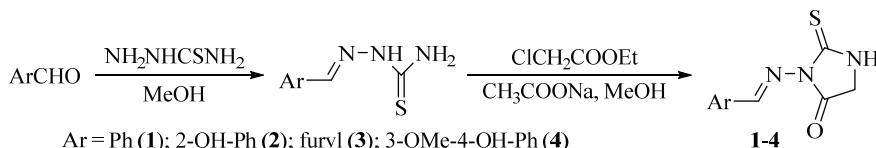
Microscopic methods

The surface morphology characterization of the MS samples was performed using a scanning electron microscope (SEM) instrument (JOEL JSM-IT300LV operated at 20 keV) after 24 h of immersion in 0.5 M HCl solution in the absence and the presence of inhibitor. Chemical composition of the samples was determined using energy dispersive X-ray spectroscopy (EDS). The EDS spectra were recorded on the X-ray spectrometer (Oxford Instruments) attached to the SEM using Aztec software. Surface characteristics of the MS samples were performed using atomic force microscopy AFM NT-MDT Solver Pro instrument in contact mode.

RESULTS AND DISCUSSION

Synthesis of inhibitors

The inhibitors were synthesized according to a previously published procedure involving thiosemicarbazide.²⁷ The first part of the synthesis is the condensation of aromatic aldehydes and thiosemicarbazide into thiosemicarbazones, which then undergo cyclization with ethyl chloroacetate in the presence of anhydrous ethyl acetate to corresponding 2-thiohydantoin derivatives in good to excellent yields (Scheme 1).



Scheme 1. Synthesis of 2-thiohydantoin-Schiff base derivatives.

Potentiodynamic polarization measurements

Potentiodynamic polarization (PP) curves for the electrochemical corrosion of MS in 0.5 M HCl without and with the inhibitors present in different concentrations are given in Fig. 2. As it can be seen from the Tafel plots, Fig. 2, the type of the polarization curves is almost the same in uninhibited and inhibited solutions. Anodic and cathodic Tafel slopes have only slight change in their values, implying that the corrosion reaction of MS is kinetics-controlled and that the adsorbed inhibitor does not affect the primary mechanism.²⁸ According to the polarization measurements, the presence of the inhibitors does not cause any significant shift in E_{corr} , but the Tafel curves were moved towards lower current densities, indicating that inhibitors can reduce the MS anodic dissolution and slow

down the hydrogen ions reduction. It can be deduced that the corrosion rate of MS in 0.5 M HCl is decreased in the presence of inhibitors in the corrosive medium. The observed decrease in corrosion current density may be ascribed to the adsorption of an inhibitor onto the MS surface. The MS surface protection from acid dissolution can be explained by the adsorption of 2-thiohydantion derivative molecules (with high negative charge density at the hetero atom) which occupy the active sites on the metal surface, mainly composed of iron atoms with incomplete d shells.^{19,21,29}

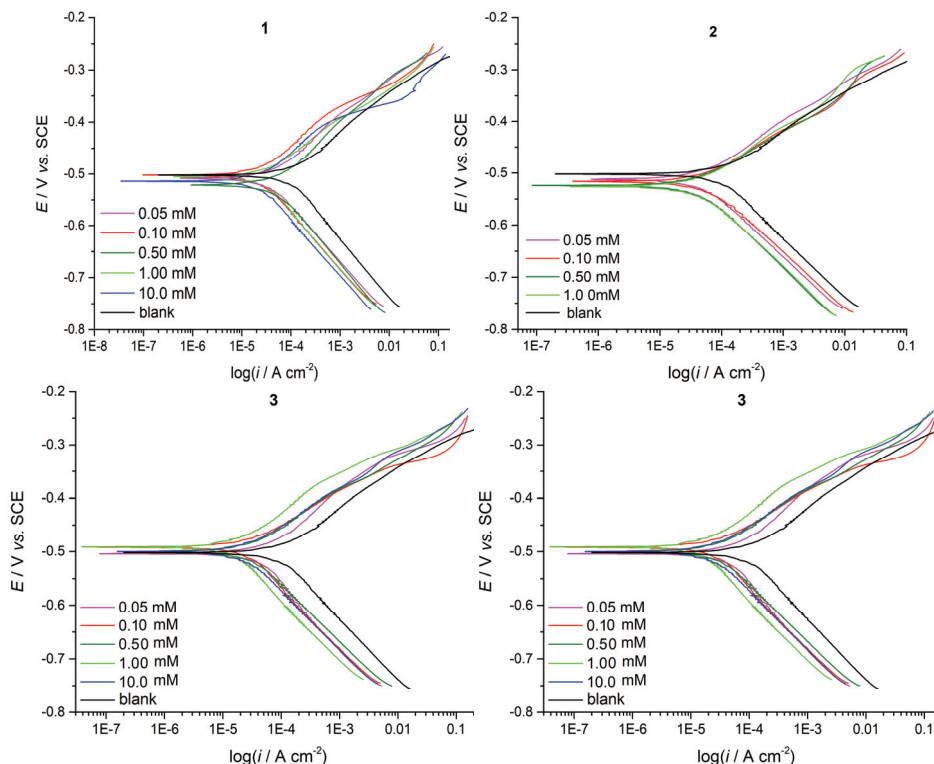


Fig. 2. The potentiodynamic polarization curves for MS in 0.5 M HCl solution in the absence and presence of inhibitor compounds **1–4**; $v = 1 \text{ mV s}^{-1}$.

Tafel extrapolations of the linear section of the anodic and cathodic curves recorded were derived and the values of the electrochemical parameters, corrosion potential (E_{corr}), corrosion current densities (i_{corr}), anodic and cathodic Tafel slopes (β_a and β_c , respectively), are listed in Table I. The corrosion potential (E_{corr}) of MS exposed to the 0.5 M HCl is about -504 mV , while in the presence of the inhibitors, E_{corr} changes from -488 to -526 mV . Determination of the inhibitor type for any of the examined compounds depends on a difference

TABLE I. Electrochemical parameters derived from the potentiodynamic polarization curves obtained for MS in 0.5 M HCl solution without and with compounds **1–4** present in various concentrations

Medium	$c_{\text{inh}} / \text{mM}$	$E_{\text{corr}} / \text{mV vs. SCE}$	$i_{\text{corr}} / \mu\text{A cm}^{-2}$	$\beta_a / \text{mV dec}^{-1}$	$\beta_c / \text{mV dec}^{-1}$	$\eta / \%$
Blank	—	—504	92	81	120	—
Compound 1	0.05	—512	38	92	110	59
	0.1	—500	23	84	112	75
	0.5	—497	26	64	113	72
	1.0	—504	26	75	117	71
	10.0	—515	21	82	105	77
	—	—	—	—	—	—
Compound 2	0.05	—515	45	92	107	51
	0.1	—514	46	74	102	50
	0.5	—521	39	74	111	58
	1.0	—526	39	84	107	58
	—	—	—	—	—	—
Compound 3	0.05	—505	45	95	141	51
	0.1	—488	23	65	113	75
	0.5	—500	23	104	73	74
	1.0	—494	17	80	115	82
	10.0	—500	24	69	113	74
	—	—	—	—	—	—
Compound 4	0.05	—510	45	111	128	51
	0.1	—490	35	67	114	62
	0.5	—511	23	88	68	75
	1.0	—510	41	82	105	55
	10.0	—513	47	76	102	49
	—	—	—	—	—	—

recorded between E_{corr} (ΔE_{corr}) in the uninhibited and the inhibited solution.^{21,29,30} If the difference ΔE_{corr} is greater than 85 mV, the inhibitor can be recognized as anodic or cathodic type, but if difference in ΔE_{corr} is lower than 85 mV, the inhibitors can be categorized as mixed type inhibitors. In our study, the shift ΔE_{corr} is less than 85 mV, indicating that the inhibition effect can be cathodic as well as anodic (mixed type inhibitors). This suggests that the presence of inhibitors in acid solutions used prevents the anodic metal dissolution reaction and controls the mechanism of cathodic hydrogen evolution at the same time. According to the PP curves recorded it can be assumed that compound **2** behaves as cathodic inhibitor reflected by decrease in the current density of the cathodic branch, and no significant effect in the anodic domain. Based on the PP curves obtained, the inhibition efficiency ($\eta / \%$) was calculated by the equation:

$$\eta = 100 \left(\frac{i_{\text{corr}}^0 - i_{\text{corr}}^i}{i_{\text{corr}}^0} \right) \quad (1)$$

where: i_{corr}^0 and i_{corr}^i are corrosion current density values recorded without and with the inhibitor present, respectively, and the results are presented in Table I. All inhibitors showed a substantial corrosion potential. The corrosion inhibition efficiency increases with increasing concentration of the 2-thiohydantoin deri-

vatives up to 1.0 mM, implying that the corrosion inhibition ability may be associated with the molecular structure of the inhibitor.

However, the additional increase in concentration up to 10.0 mM for compounds **3** and **4** resulted in the reduction of the inhibition efficiency. Recently, Alhaffar *et al.*³¹ and Pavithra *et al.*³² reported analogous behaviour of inhibitors in 1.0 M HCl and 0.5 M H₂SO₄. They assumed that after specific inhibitor quantity increments in solution, when optimum inhibitor concentration is achieved, no active sites remained for adsorption, because maximum surface coverage is accomplished, and the inhibitor molecules could not adsorb on the substrate. However, the corrosion still occurs, probably because the interactions among adsorbed and unadsorbed inhibitor molecules generate the desorption of molecules which results in reduced inhibition efficiency, with the additional increasing in concentration of inhibitors. For all studied inhibitors, the recorded corrosion inhibition is relatively stable at concentration around 0.5 mM, with the corrosion inhibition rate of \approx 75 %. The mechanism of inhibition depends on the interaction between the inhibitor and the metal surface. It is known that organic corrosion inhibitors have at least one polar unit with heteroatoms (nitrogen, sulfur, oxygen and sometimes phosphorus) which is considered as the reaction centre for chemisorption processes. Additionally, the size, orientation, shape and electric charge on the inhibitor molecule determine the degree of adsorption and the inhibition effectiveness. Moreover, iron possesses great coordination affinity to heteroatom containing ligands. All these factors could explain the difference in the inhibiting action of the thiohydantoin-Schiff base derivatives. All compounds have four chelating sites ($-\text{NH}$, C=S, C=N and aromatic ring). The obtained results indicate that all compounds adhere to the chemisorption process through the adsorption on the MS surface established on the donor–acceptor interactions between the π electrons of donor atoms of the inhibitors and the vacant d orbitals of the ferric ion in the oxidized MS surface.^{21,23} However, compound **3** exhibited the best performances with the inhibition rate of 82 %. This higher inhibitions efficiency might be attributed to the presence of an additional oxygen atom in the heteroaromatic ring, which contributed to better adsorbing.²⁰

Potentiostatic electrochemical impedance spectroscopy

Potentiostatic electrochemical impedance spectroscopy (PEIS) was used for the estimation of the performance ability rate, characterization of the various corrosion processes and the study of the reaction mechanisms at the electrochemical interface. After PP studies, the best performing concentrations of all 2-thiohydantoin derivatives were used for further PEIS evaluation. Fig. 3 illustrates the Nyquist plots of the MS electrode in a 0.5 M HCl solution in the absence and the presence of different inhibitor (compounds **1**–**4**) concentrations. Since the potentiodynamic measurements showed that compound **2** has the smallest corrosion inhi-

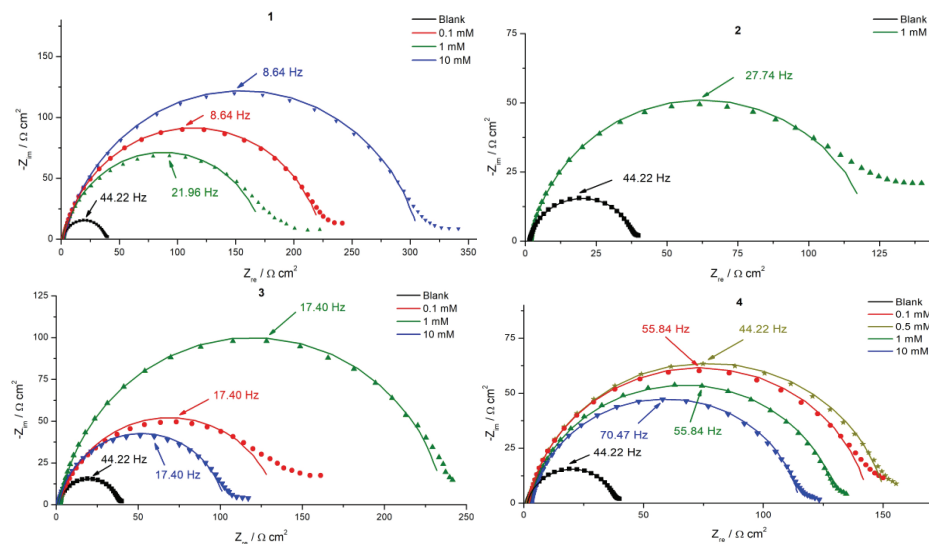


Fig. 3. Nyquist plots for MS electrode and different inhibitor compounds **1–4** at various concentrations with respect to blank 0.5 M HCl. Scattered dots represent experimental data, while solid lines represent calculated and fitted results.

bition efficiency among all tested, only the best performing concentration (1.0 mM, $\eta = 58\%$, Table I) was used for further PEIS evaluation. The presence of different inhibitors causes an increase in the capacitive loops, compared to the reference solution. Taking into consideration the shape of the impedance diagram, it can be said that their size depends on both structure and concentration of the inhibitor and that the Nyquist representations spectra consist of one single slightly depressed capacitive loop, showing that the charge transfer controls the corrosion reaction on an inhomogeneous and rough electrode surface.³³ Analysis of Nyquist plots reveals that the capacitive loops are depressed semicircles and not perfect semicircles, as expected from theory of PEIS, that accounts for frequency dispersion effect of a rough and inhomogeneous electrode surface, where the inhibitor molecular film is not acting as a perfect double layer capacitor. The results can be interpreted in terms of an equivalent circuit of the electrical double layer shown in Fig. 4. This equivalent circuit has been used to model the interface between iron and acid.³⁴ The double layer capacitance, C_{dl} was calculated using the following equation:^{35,36}

$$C_{dl} = \left(\frac{1}{2\pi f(-Z''_{max}) R_{ct}} \right) \quad (2)$$

where: C_{dl} / F cm⁻² is the double layer capacitance, $-Z''_{max}$ is the maximum imaginary component of the impedance, R_s / Ω cm² is the uncompensated solution resistance and R_{ct} / Ω cm² is the charge transfer resistance.

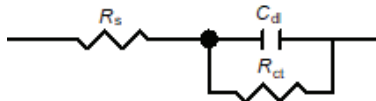


Fig. 4. Randle's equivalent circuit used for fitting of the PEIS curves.

The electrochemical data was evaluated using a Randle's equivalent circuit (Fig. 4) where R_s is the solution resistance, C_{dl} is the double layer capacitance and R_{ct} is the charge transfer resistance.^{36,37}

The proposed equivalent circuit and the fitted results represent a good match, which is proved by very small chi-square values that are in the order of 10^{-3} for all the experimental data. All electrochemical impedance parameters are presented in Table II. As corrosion current (i_{corr}) is inversely related to R_{ct} , the inhibition efficiency, performance ability (η / %) can be determined by the following expression:^{28,29}

$$\eta = 100 \left(1 - \frac{R_{ct}^0}{R_{ct}} \right) \quad (3)$$

where: R_{ct}^0 and R_{ct} are the charge transfer resistances of uninhibited and inhibited solutions.

Data clearly shows that R_{ct} has an ascending trend, whereas C_{dl} has a descending trend at the whole concentration range. The decrease in C_{dl} values can be attributed to a decrease in local dielectric constant and, more likely, to an increase in the thickness of electrical double layer. This suggests that the inhibitor molecules inhibit the corrosion rate by adsorption at metal/solution interface.³⁸ The concentration of the inhibitor plays a crucial role, but it cannot be stated that for all the inhibitors there is a positive shift in the R_{ct} values with the increasing concentration. This shift in R_{ct} clearly shows the increasing inhibition efficiency and it may be attributed to the blocking of active sites of the metal surface by surface adsorption. The capacitance values showed a reduction due to decrease in the electric double layer, which is probably due to the replacement of water molecules, which have a higher dielectric constant, with inhibitor molecules possessing a lower dielectric constant, hence supporting the idea of surface adsorption of inhibitor molecules.³⁷ R_s refers to the solution resistance and its values increase noticeably only when compound 4 was used as an inhibitor.

The inhibitors were also analysed by Bode diagrams (Supplementary material, Fig. S-13). Bode diagrams of all inhibitor concentrations, as well as untreated MS electrode show phase shift that corresponds to the maximum of the

semi-circle presented in Nyquist diagram. This is typical behaviour for the process that is represented by Randle's equivalent circuit shown in Fig. 4. There is slight, but not significant, shift in the frequency for maximum phase shift, which could be due to different types of inhibitors, and not due to different mechanisms. The mechanism of corrosion inhibition is based on the adsorption of inhibitor on the MS electrode surface.

TABLE II. Electrochemical impedance parameters in absence and in the presence of inhibitors

Medium	c_{inh} / mM	R_s / $\Omega \text{ cm}^2$	R_{ct} / $\Omega \text{ cm}^2$	C_{dl} / $\mu\text{F cm}^{-2}$	η / %
Blank	—	2.86	82.3	987.2	—
Compound 1	0.05	—	—	—	—
	0.1	2.31	433	38.2	81
	0.5	—	—	—	—
	1.0	2.64	343	49.4	76
	10. 0	2.19	748	31.4	89
Compound 2	0.05	—	—	—	—
	0.1	—	—	—	—
	0.5	—	—	—	—
	1.0	3.01	187	118.4	56
	10. 0	—	—	—	—
Compound 3	0.05	—	—	—	—
	0.1	2.75	329	47.6	75
	0.5	—	—	—	—
	1.0	2.87	633	34.8	87
	10. 0	3.14	211	98.1	61
Compound 4	0.05	—	—	—	—
	0.1	2.56	294	55.8	72
	0.5	3.26	317	51.2	74
	1.0	3.55	257	66.9	68
	10. 0	2.98	305	76.5	63

Gravimetric measurements

Immersion test followed by the weight loss method is one of the cheapest, easiest, and most widely recognized strategies to explore and calculate the corrosion rate. The influence of varying concentrations of compound **3** on corrosion of MS in aggressive test solutions was studied by the weight loss method, and the obtained results of inhibition efficiencies and corrosion rates are presented in Table III. The inhibition efficiencies of compound **3** increase with its concentration, which may be ascribed to greater coverage of the metal surface with inhibitor molecules. From the weight loss, the corrosion rate (CR) and the inhibition efficiency (η / %) were estimated as:^{33,39}

$$CR = \frac{w_I - w_F}{St} \quad (4)$$

where, w_I and w_F are the initial and the final weights (mg) of MS, S / cm^2 is the surface of the MS sample exposed to the test solution, and t / h is the immersion time.

$$\eta = 100 \left(\frac{CR_0 - CR}{CR_0} \right) \quad (5)$$

where CR and CR_0 are the corrosion rates in the presence and the absence of compound **3**, respectively.

TABLE III. Corrosion parameters for MS sample after immersion for 24 h in 0.5 M HCl solution in the absence and presence of compound **3** at different concentrations.

Medium	$c_{\text{inh}} / \text{mM}$	$CR / \text{mg cm}^{-2} \text{h}^{-1}$	$\eta / \%$
Blank	—	0.659	—
Compound 3	0.1	0.268	59
	1.0	0.075	89
	10.0	0.066	90

Surface study

Corrosion of the MS surface was characterized after immersion in 0.5 M HCl solution with and without inhibitor compound **3** using SEM/EDS technique. SEM was used for surface morphology while EDS provided data about the elemental composition. Fig. 5 illustrates SEM images of the uninhibited and the inhibited MS surfaces after immersion for 24 h in 0.5 M HCl solution. Surface of the MS sample directly exposed to free acid without the presence of inhibitors is severely damaged and rough with deep corrosion cracks and pits (Fig. 5A), while the surface of the sample submersed in the acid solution with the compound **3** at 1 mM was uniform, smoother and less corroded and cracked (Fig. 5B). The SEM surface analysis are in good agreement with corrosion metal evaluation and showed that the compound **3** has good inhibition properties and protects the MS surface from the effects of acid by the formation of the protective film on the metallic surface.⁴⁰

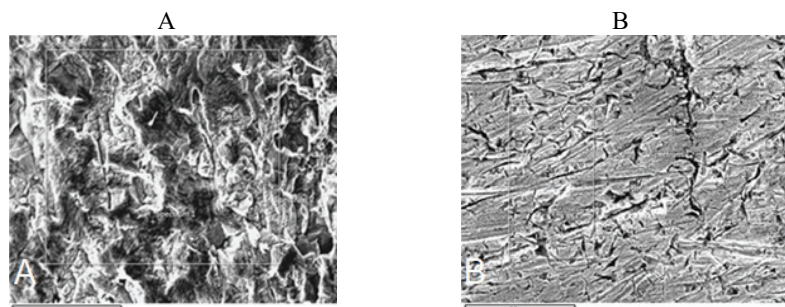


Fig. 5. SEM images of the MS sample without (A) and with inhibitor compound **3** at 1 mM (B).

EDS analysis of both MS samples (without and with the addition of compound **3**) was performed to record elemental compositions. EDS analysis of the MS samples without the inhibitor compound **3** showed the presence of high content of oxygen (9.67 %). On the other hand, EDS analysis of the sample immersed in the solution with the inhibitor compound **3** showed a significant influence of its presence on the corrosion of the sample, since the oxygen content was reduced to only 0.12 %, obviously due to the formation of thin protective layer of inhibitor molecules on the MS surface. This protective film was also responsible for the inhibition of corrosion.⁴¹

The 3D micrographs of MS surfaces acquired from AFM without and with the compound **3** are displayed in Fig. 6. Fig. 6A shows MS surface after immersion in 0.5 M HCl solution without the inhibitor with average roughness of 337 nm. It should be noted that the roughness parameters of the sample are much higher and that the peak heights of the roughness profile exceed the measuring range, so the sampling area where the heights are smaller and the surface is more uniform was selected for analysis. Fig. 6B shows MS surface immersed in the solution with the inhibitor compound **3** with the average roughness of 97.5 nm, suggesting good adsorption on the metal surface.

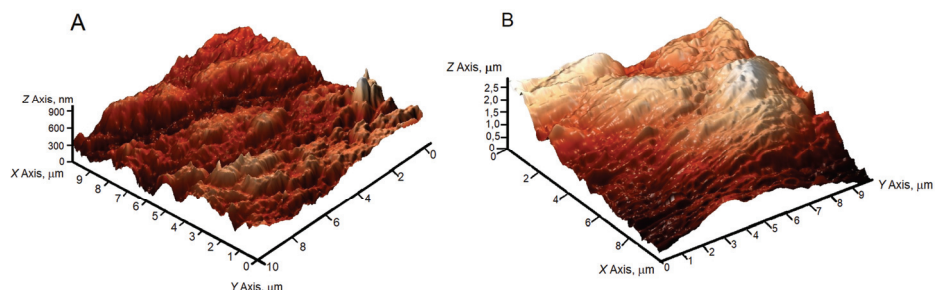


Fig. 6. AFM images of MS without (A) and with inhibitor compound **3** (B).

CONCLUSION

Four 2-thiohydantoin–Shiff base derivatives were synthesized as eco-friendly corrosion inhibitors and evaluated for their anti-corrosion performance for MS in 0.5 M HCl solution. The corrosion inhibition efficiency of all inhibitors increases with their concentration reaching a maximum value at 1.0 mM. The polarization curves reveal that the thiohydantoin derivatives act as mixed type inhibitors. The derivative with a heteroaryl furyl group, compound **3**, is the most effective inhibitor, exhibiting the inhibition efficiency in the range from 82–90 % depending on the method used. The changes in impedance parameters indicate the adsorption of inhibitors on the MS surface and thus formation of a protective film. SEM and AFM confirmed the presence of the inhibitor protective film on the MS surface. The present investigation has shown that these low cost and environment-

ally friendly inhibitors provide good protection for mild steel against corrosion in the acidic medium.

SUPPLEMENTARY MATERIAL

Additional data and information are available electronically at the pages of journal website: <https://www.shd-pub.org.rs/index.php/JSCS/article/view/11776>, or from the corresponding author on request.

Acknowledgement. The authors are grateful for financial support from The Ministry of Education, Science and Technological Development of Republic of Serbia (Agreement Nos: 451-03-68/2022-14/200378, 451-03-68/2022-14/200026 and 451-03-68/2022-14/200052).

ИЗВОД

АНТИКОРОЗИОНА АКТИВНОСТ ДЕРИВАТА ШИФОВИХ БАЗА 2-ТИОХИДАНТОИНА ЗА МЕКИ ЧЕЛИК У 0,5 М HCl

ПЕТАР Б. СТАНИЋ¹, НАТАША М. ВУКИЋЕВИЋ², ВЕСНА С. ЦВЕТКОВИЋ², МИРОСЛАВ М. ПАВЛОВИЋ²,
СИЛВАНА Б. ДИМИТРИЈЕВИЋ³, БИЉАНА ШМИТ¹ и МАРИЈА Д. ЖИВКОВИЋ⁴

¹Институј за информационе технологије Краљевачи, Универзитет у Краљевцу, Јована Цвијића бб,
34000 Краљевачи, ²Институј за хемију, технологију и металургију, Универзитет у Београду,
Његошева 12, 11000 Београд, ³Институј за рударство и металургију Бор, Зелени булевар 35,
19210 Бор и ⁴Факултет медицинских наука, Универзитет у Краљевцу, Светозара
Марковића 69, 34000 Краљевачи

Неколико деривата Шифових база 2-тиохидантоина су направљени као еколошки прихватљиви инхибитори корозије меког челика у киселој средини. Њихова антикорозиона својства су испитана на меком челику у 0,5 M раствору HCl као корозионом електролиту, користећи уобичајене гравиметријске и различите електрохемијске технике (мерење губитка масе, потенциодинамичка поларизација, потенциостатска спектроскопија електрохемијске импеданције). Површина меког челика је окарактерисана двема аналитичким техникама, скенирајућом електронском микроскопијом за морфологију површине и елементарни састав и микроскопијом атомске силе. Студија је показала да се инхибиторно деловање ових еколошки бенигних инхибитора, синтетисаних из јефтиних комерцијално доступних полазних материјала, може приписати адсорпцији инхибитора на површини меког челика.

(Примљено 12. априла, ревидирано 12. јула, прихваћено 24. августа 2022)

REFERENCES

1. G. Koch, J. Varney, N. Thompson, O. Moghissi, M. Gould, J. Payer, *NACE Int.* (2016) (<http://impact.nace.org/documents/Nace-International-Report.pdf>)
2. D. Dwivedi, K. Lepková, T. Becker, *RSC Adv.* **7** (2017) 4580 (<https://www.doi.org/10.1039/C6RA25094G>)
3. T. J. Harvey, F. C. Walsh, A. H. Nahle, *J. Mol. Liq.* **266** (2018) 160 (<https://www.doi.org/10.1016/j.molliq.2018.06.014>)
4. D. Douche, H. Elmsellem, E. H. Anouar, L. Guo, B. Hafez, B. Tüzün, A. El Louzi, K. Bougrin, K. Karrouchi, B. Himmé, *J. Mol. Liq.* **308** (2020) 113042 (<https://www.doi.org/10.1016/j.molliq.2020.113042>)
5. A. Y. Musa, A. A. H. Kadhum, M. S. Takriff, A. R. Daud, S. K. Kamarudin, N. Muhamad, *Corros. Eng. Sci. Technol.* **45** (2010) 163 (<https://www.doi.org/10.1179/147842208X386359>)

6. N. Errahmany, M. Rbaa, A. S. Abousalem, A. Tazouti, M. Galai, E. H. El Kafssaoui, M. E. Touhami, B. Lahrissi, R. Touir, *J. Mol. Liq.* **312** (2020) 113413 (<https://www.doi.org/10.1016/j.molliq.2020.113413>)
7. E. Akbas, E. Yildiz, A. Erdogan, *J. Serb. Chem. Soc.* **85** (2020) 481 (<https://www.doi.org/10.2298/JSC190326081A>)
8. F. Bentiss, M. Lagrenée, *J. Mater. Environ. Sci.* **2** (2011) 13 (<https://www.jmaterenvironsci.com/Document/vol2/3-JMES-62-2011-Bentiss2.pdf>)
9. K. Tamalmani, H. Husin, *Appl. Sci.* **10** (2020) 3389 (<https://www.doi.org/10.3390/APP10103389>)
10. G. Gece, *Corros. Sci.* **53** (2011) 3873 (<https://www.doi.org/10.1016/j.corsci.2011.08.006>)
11. C. Verma, E. E. Ebenso, M. A. Quraishi, C. M. Hussain, *Mater. Adv.* **2** (2021) 3806 (<https://www.doi.org/10.1039/d0ma00681e>)
12. V. Saraswat, M. Yadav, I. B. Obot, *Colloids Surfaces, A* **599** (2020) 124881 (<https://www.doi.org/10.1016/j.colsurfa.2020.124881>)
13. Y. Abboud, O. Tanane, A. El Bouari, R. Salghi, B. Hammouti, A. Chetouani, S. Jodeh, *Corros. Eng. Sci. Technol.* **51** (2016) 557 (<https://www.doi.org/10.1179/1743278215Y.0000000058>)
14. M. Rbaa, F. Benhiba, P. Dohare, L. Lahrissi, R. Touir, B. Lahrissi, A. Zarrouk, Y. Lahrissi, *Chem. Data Collect.* **27** (2020) 100394 (<https://www.doi.org/10.1016/j.cdc.2020.100394>)
15. N. Y. Silvère Diki, N. H. Coulibaly, K. F. Kassi, A. Trokourey, *J. Electrochem. Sci. Eng.* **11(2)** (2021) 97-106 (<https://doi.org/10.5599/jese.952>)
16. F. E. Abeng, V. Anadebe, P. Y. Nkom, K. J. Uwakwe, E. G. Kamalu, *J. Electrochem. Sci. Eng.* **11(1)** (2021) 11 (<https://doi.org/10.5599/jese.887>)
17. M. A. Metwally, E. Abdel-Latif, *J. Sulfur Chem.* **33** (2012) 229 (<https://www.doi.org/10.1080/17415993.2011.643550>)
18. S. H. Cho, S. H. Kim, D. Shin, *Eur. J. Med. Chem.* **164** (2019) 517 (<https://www.doi.org/10.1016/j.ejmech.2018.12.066>)
19. L. H. Madkour, A. M. Hassanein, M. M. Ghoneim, S. A. Eid, *Monatsh. Chem.* **132** (2001) 245 (<https://doi.org/10.1007/s007060170134>)
20. L. O. Olasunkanmi, B. P. Moloto, I. B. Obot, E. E. Ebenso, *J. Mol. Liq.* **252** (2018) 62 (<https://www.doi.org/10.1016/j.molliq.2017.11.169>)
21. A. O. Yüce, G. Kardaş, *Corros. Sci.* **58** (2012) 86 (<https://www.doi.org/10.1016/j.corsci.2012.01.013>)
22. A. O. Yüce, E. Telli, B. D. Mert, G. Kardaş, B. Yazıcı, *J. Mol. Liq.* **218** (2016) 384 (<https://www.doi.org/10.1016/j.molliq.2016.02.087>)
23. M. S. Kumar, S. L. A. Kumar, A. Sreekanth, *Ind. Eng. Chem. Res.* **51** (2012) 5408 (<https://www.doi.org/10.1021/ie203022g>)
24. M. Chafiq, A. Chaouiki, H. Lgaz, R. Salghi, S. L. Gaonkar, K. S. Bhat, R. Marzouki, I. H. Ali, M. I. Khan, H. Shimizu, I. M. Chung, *J. Adhes. Sci. Technol.* **34** (2020) 1283 (<https://www.doi.org/10.1080/01694243.2019.1707561>)
25. R. Kumar, H. Kim, G. Singh, *J. Mol. Liq.* **259** (2018) 199 (<https://www.doi.org/10.1016/j.molliq.2018.02.123>)
26. S. T. Arab, *Mater. Res. Bull.* **43** (2008) 510 (<https://www.doi.org/10.1016/j.materresbull.2007.10.025>)
27. B. Šmit, R. Z. Pavlović, A. Radosavljević-Mihailović, A. Došen, M. G. Ćurčić, D. S. Šeklić, M. N. Živanović, *J. Serb. Chem. Soc.* **78** (2013) 217 (<https://www.doi.org/10.2298/JSC120725154S>)

28. M. Elfaydy, H. Lgaz, R. Salghi, M. Larouj, S. Jodeh, M. Rbaa, H. Oudda, K. Toumiat, B. Lakhrissi, *J. Mater. Environ. Sci.* **7** (2016) 3193 (https://www.jmaterenvironsci.com/Document/vol7/vol7_N9/333-JMES-2379-ELfaydy.pdf)
29. S. Fatima, R. Sharma, F. Asghar, A. Kamal, A. Badshah, H. B. Kraatz, *J. Ind. Eng. Chem.* **76** (2019) 374 (<https://www.doi.org/10.1016/j.jiec.2019.04.003>)
30. M. El Faydy, B. Lakhrissi, A. Guenbour, S. Kaya, F. Bentiss, I. Warad, A. Zarrouk, *J. Mol. Liq.* **280** (2019) 341 (<https://www.doi.org/10.1016/j.molliq.2019.01.105>)
31. M. T. Alhaffar, S. A. Umoren, I. B. Obot, S. A. Ali, *RSC Adv.* **8** (2018) 1764 (<https://doi.org/10.1039/C7RA11549K>)
32. M. K. Pavithra, T. V. Venkatesha, K. Vathsala, K. O. Nayana, *Corros. Sci.* **52** (2010) 3811 (<https://doi.org/10.1016/j.corsci.2010.07.034>)
33. M. El Faydy, M. Rbaa, L. Lakhrissi, B. Lakhrissi, I. Warad, A. Zarrouk, I. B. Obot, *Surf. Interfaces* **14** (2019) 222 (<https://www.doi.org/10.1016/j.surfin.2019.01.005>)
34. A. Yousefi, S. Javadian, N. Dalir, J. Kakemam, J. Akbari, *RSC Adv.* **5** (2015) 11697 (<https://www.doi.org/10.1039/c4ra10995c>)
35. M. A. Hegazy, H. M. Ahmed, A. S. El-Tabei, *Corros. Sci.* **53** (2011) 671 (<https://www.doi.org/10.1016/j.corsci.2010.10.004>)
36. I. Ahamad, M. A. Quraishi, *Corros. Sci.* **51** (2009) 2006 (<https://www.doi.org/10.1016/j.corsci.2009.05.026>)
37. E. Mccafferty, N. Hackerman, *J. Electrochem. Soc.* **119** (1972) 146 (<https://doi.org/10.1149/1.2404150>)
38. M. Quraishi, J. Rawat, *Mater. Chem. Phys.* **70** (2001) 95 ([https://www.doi.org/10.1016/S0254-0584\(00\)00459-4](https://www.doi.org/10.1016/S0254-0584(00)00459-4))
39. R. Hsissou, O. Dagdag, S. Abbout, F. Benhiba, M. Berradi, M. El Bouchti, A. Berisha, N. Hajjaji, A. Elharfi, *J. Mol. Liq.* **284** (2019) 182 (<https://www.doi.org/10.1016/j.molliq.2019.03.180>)
40. P. Muthukrishnan, B. Jeyaprabha, P. Prakash, *Arab. J. Chem.* **10** (2017) S2343 (<https://www.doi.org/10.1016/j.arabjc.2013.08.011>)
41. K. Kansal, R. Chopra, R. Kumar, A. Kumar, B. Yadav, R. Kishore Sharma, G. Singh, *Indian J. Chem. Technol.* **24** (2017) 169 (<http://op.niscair.res.in/index.php/IJCT/article/view/13124>).